ACS chemical biology

Articles

pubs.acs.org/acschemicalbiology

Tetraterpene Synthase Substrate and Product Specificity in the Green Microalga *Botryococcus braunii* Race L

Hem R. Thapa,[†,§] Su Tang,[†] James C. Sacchettini,[†,‡] and Timothy P. Devarenne*[,†]

[†]Department of Biochemistry & Biophysics, Texas A&M University, College Station, Texas 77843, United States

[‡]Department of Chemistry, Texas A&M University, College Station, Texas 77843, United States

Supporting Information

ABSTRACT: Recently, the biosynthetic pathway for lycopadiene, a C_{40} tetraterpenoid hydrocarbon, was deciphered from the L race of *Botryococcus braunii*, an alga that produces hydrocarbon oils capable of being converted into combustible fuels. The lycopadiene pathway is initiated by the squalene synthase (SS)-like enzyme lycopaoctaene synthase (LOS), which catalyzes the head-to-head condensation of two C_{20} geranylgeranyl diphosphate (GGPP) molecules to produce C_{40} lycopaoctaene. LOS shows unusual substrate promiscuity for SS or SS-like enzymes by utilizing C_{15} farnesyl diphosphate (FPP) and C_{20} phytyl diphosphate in addition to GGPP as substrates. These three substrates can be combined by LOS individually or in combinations to produce six different hydrocarbons of C_{30}, C_{35}, and C_{40} chain lengths. To understand LOS substrate and product specificity, rational mutagenesis experiments were conducted based on sequence alignment with several SS proteins as well as a structural comparison with the human SS (HSS) crystal structure. Characterization of the LOS mutants *in vitro* identified Ser276 and Ala288 in the LOS active site as key amino acids responsible for controlling substrate binding, and thus the promiscuity of this enzyme. Mutating these residues to those found in HSS largely converted LOS from lycopaoctaene production to C_{30} squalene production. Furthermore, these studies were confirmed *in vivo* by expressing LOS in *E. coli* cells metabolically engineered to produce high FPP and GGPP levels. These studies also offer insights into tetraterpene hydrocarbon metabolism in *B. braunii* and provide a foundation for engineering LOS for robust production of specific hydrocarbons of a desired chain length.

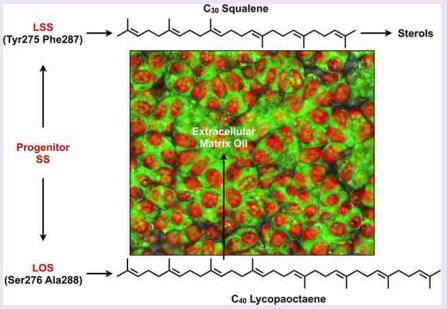

Isoprenoids (a.k.a. terpenes) are one of the largest groups of structurally diverse natural products produced by all domains of life and are biosynthesized *via* either the mevalonate pathway or the methylerythritol phosphate (MEP) pathway depending on the organism in question.[1] Besides critical roles in primary and secondary metabolism, isoprenoids and derivatives have a wide range of applications including use as medicines, nutraceuticals, agricultural chemicals, fragrances, flavorings, and industrial chemicals.[2] More recently, there has been significant interest in the use and development of isoprenoid-based chemicals as a direct substitute for petroleum-derived fuels since the physicochemical characteristics of some isoprenoids make them ideal for use as combustion fuels.[3,4] However, low yields in natural hosts have directed isoprenoid-based biofuel research toward metabolic engineering for overproduction of isoprenoid chemicals in industrial microorganisms such as yeast and *E. coli*.[3,5]

The colony-forming green microalga *Botryococcus braunii* is an exception to low isoprenoid yielding organisms as it naturally produces large amounts of liquid hydrocarbon oils, which are stored in the colony extracellular matrix.[6] These hydrocarbons can be catalytically cracked to produce petroleum-equivalent combustion engine fuels,[7,8] making *B. braunii* hydrocarbons a promising renewable biofuel feedstock.[8,9] There are three chemical races of *B. braunii*, races A, B, and L, each producing distinct types of hydrocarbons.[6] Race L, the focus of this study, produces the MEP pathway derived C_{40} tetraterpene hydrocarbon lycopadiene as the predominant hydrocarbon.[10,11]

The major intermediates and the key enzyme for the lycopadiene biosynthetic pathway have recently been identified in the L race of *B. braunii*.[12] This enzyme, termed lycopaoctaene synthase (LOS), catalyzes a two-step reaction resembling that of squalene synthase (SS).[12] In the first step of the SS reaction, two molecules of C_{15} farnesyl diphosphate (FPP) are condensed head-to-head to generate the intermediate presqualene diphosphate (PSPP), which is reductively rearranged to squalene in the second reaction step (Figure 1).[13] Squalene is then used for sterol production. By comparison, in the LOS reaction two molecules of C_{20} geranylgeranyl diphosphate (GGPP) undergo head-to-head dimerization to produce the prelycopaoctaene diphosphate (PLPP) intermediate in the first step, followed by reductive rearrangement to produce C_{40} lycopaoctaene in the second step (Figure 1).[12] Production of lycopaoctaene represents the committed step in

Received: June 1, 2017
Accepted: August 16, 2017
Published: August 16, 2017

DOI: 10.1021/acschembio.7b00457
ACS Chem. Biol. 2017, 12, 2408−2416

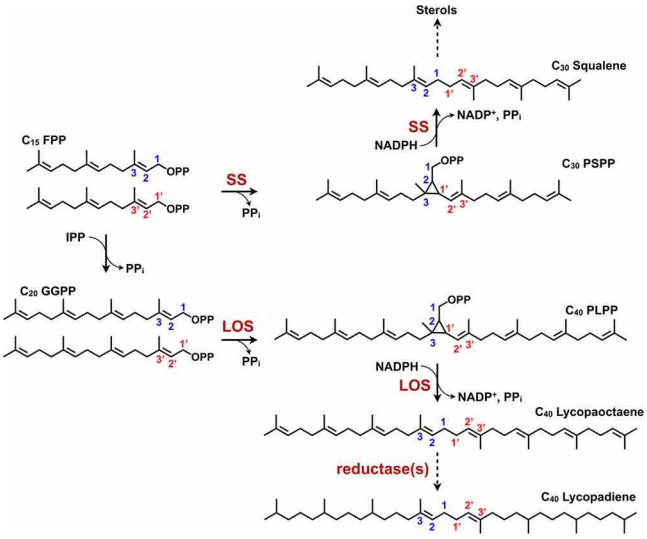

Figure 1. Squalene production and lycopadiene biosynthesis in *Botryococcus braunii* race L. Two molecules of farnesyl diphosphate (FPP) are condensed by squalene synthase (SS) to produce the presqualene diphosphate (PSPP) intermediate followed by reductive rearrangement to produce squalene. Lycopaoctaene synthase (LOS) catalyzes the condensation of two molecules of geranylgeranyl diphosphate (GGPP) to produce the prelycopaoctaene diphosphate (PLPP) intermediate followed by reductive rearrangement to produce lycopaoctaene, which is subsequently reduced to produce lycopadiene.

lycopadiene biosynthesis and is subsequently reduced to lycopadiene by a yet to be identified enzyme(s) (Figure 1).[12]

The LOS enzyme also shows unusual substrate promiscuity not previously observed in eukaryotic SS or SS-like enzymes.[12] LOS is capable of utilizing three prenyl diphosphate substrates, FPP, GGPP, and C_{20} phytyl diphosphate (PPP), individually or in combination to produce six different hydrocarbons with C_{30}, C_{35}, and C_{40} chain lengths.[12] For example, when FPP and GGPP are provided as equimolar substrates, LOS produces three of these hydrocarbons: squalene from combining two FPP molecules, $C_{35}H_{58}$ from joining one FPP and one GGPP, and lycopaoctaene from the condensation of two GGPP molecules.[12] The remaining three hydrocarbons are produced when LOS is incubated with FPP and PPP or GGPP and PPP (Figure S1).[12] This discovery provides a unique opportunity to engineer the LOS enzyme for robust production of individual hydrocarbons with specific chain lengths for possible industrial uses such as fuel production.

In order to accomplish this, the mechanism underlying LOS substrate promiscuity needs to be understood. It has been proposed that LOS and the *B. braunii* L race SS (LSS) arose from an ancient *SS* gene duplication, with LSS maintaining SS activity, while LOS evolved the new catalytic function to produce lycopaoctaene leading to hydrocarbon production.[12] The promiscuous LOS activity is likely due to preservation of the original SS activity following the gene duplication event.[12] Thus, conversion of LOS to an enzyme producing only one C_{30}, C_{35}, or C_{40} hydrocarbon product for potential industrial use could be accomplished by understanding how LOS binds substrate for product formation. In this study, we use protein alignments between LOS and SS proteins, as well as a comparison of a predicted LOS 3D strucure with the human SS crystal structure to conduct rational site-directed mutagenesis in order to identify the critical LOS residues important for conferring substrate and product specificity.

RESULTS AND DISCUSSION

LOS Sequence and Structural Comparison to SS Proteins. Initially, LOS was compared to LSS and four other SS enzymes to determine regions of similarity or dissimilarity and to identify mutational targets for understanding LOS substrate specificity. The SS catalyzed reaction has been extensively investigated due to consideration of human SS (HSS) as a drug target for reducing serum cholesterol levels,[14−16] and the role of important catalytic residues has been verified.[14−17] From these studies, seven functional SS domains have been identified: domains I−V for substrate binding and catalysis and a FLAP domain and a J-K loop involved in NADPH binding (Figure S2).[15,17,18] The alignment of LOS with the five SS proteins showed conservation of all these domains in LOS (Figure S2), making it difficult to use these alignments alone to identify residues conferring LOS substrate specificity. Additionally, residues dictating the promiscuity of LOS may lie outside these conserved regions.

Thus, a structural comparison was used to identify the amino acids that control LOS substrate binding. To do this, a predicted LOS structure was generated that showed LOS as an α-helical protein with several regions matching previous SS structures such as a large catalytic channel running through the center of the protein (dashed box in Figure S3A), an N-terminal flexible region (green in Figure S3A), and a C-terminal transmembrane domain (magenta in Figure S3A).

While there have been several SS and SS-like structures determined,[14−16,19,20] the HSS crystal structure, specifically a truncated HSS^{31-370} protein in complex with the FPP analog farnesyl thiodiphosphate (FSPP),[15] was chosen for comparison to the predicted LOS structure. This HSS^{31-370} protein retains full SS activity and was generated by deleting the N-terminal flexible hydrophobic region and the C-terminal transmembrane domain.[15] As we previously reported,[12] a similar LOS C-terminal truncation, producing LOS^{1-391}, maintained full enzyme activity (Figure S3B). In order to match the HSS^{31-370} structure, N- and C-terminal truncations were made to LOS^{1-391} to generate LOS^{33-381} (Figure S3C), which had a marginal reduction in enzyme activity (Figure S3B,D). This suggests a comparison of LOS^{33-381} to HSS^{31-370} should offer valuable information regarding potential LOS substrate binding sites as both structures superimpose very well (Figure S3C).

Identification of LOS Residues for Mutagenesis. Based on the HSS^{31-370}–LOS^{33-381} structural comparison, five LOS amino acids appear to be important for substrate interaction: Thr65, Met180, Ser276, Ala288, and Val289 (Figure 2A). Except for Ser276, all residues are located within the conserved functional SS domains I, III, and IV, and all five LOS residues are different from the corresponding amino acids in the other SS proteins (Figure 2A). For instance, the corresponding HSS amino acids are Val69, Leu183, Tyr276, Phe288, and Cys289 (Figure 2A), all of which have been shown to form a hydrophobic floor in the central cavity of the HSS active site for interaction with the nonpolar FSPP tails.[15] The hydrophobic side chains of Val69, Leu183, and Phe288 form the hydrophobic floor for the substrate 1 (S1) pocket, whereas the hydrophobic portions of the Tyr276 and Cys289 side chains form the hydrophobic floor for the substrate 2 (S2) pocket (Figure 2B). The corresponding five LOS residues are located in the same hydrophobic region of the LOS active site, with the Thr65, Met180, and Ala288 side chains contributing to the S1

DOI: 10.1021/acschembio.7b00457
ACS Chem. Biol. 2017, 12, 2408−2416

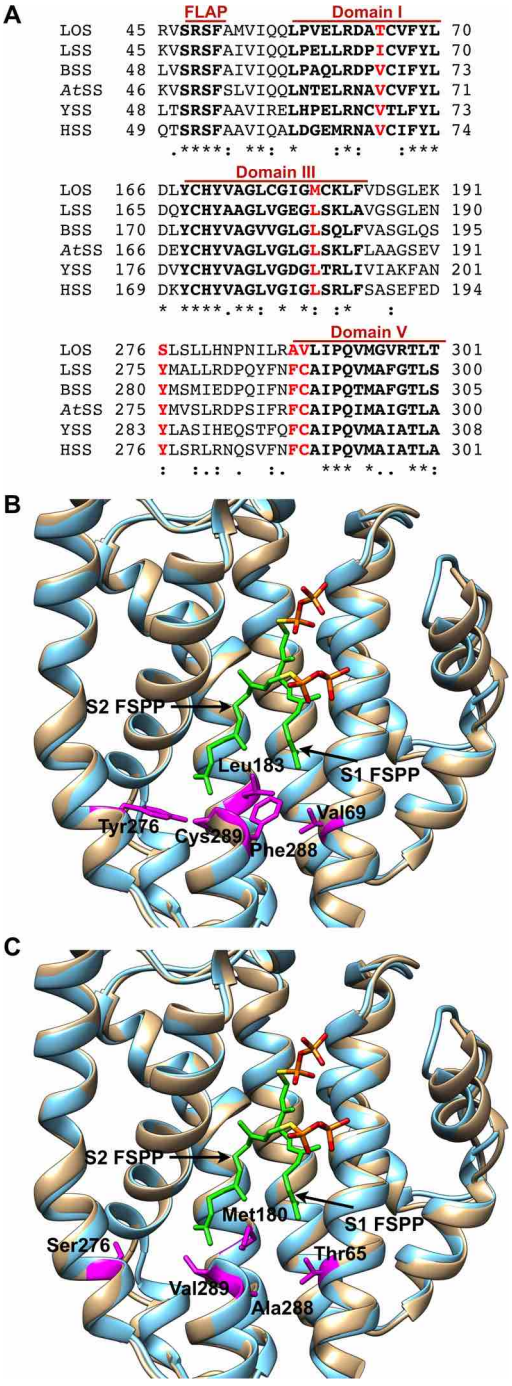

Figure 2. Amino acid sequence alignment and superposition of the HSS crystal structure bound to farnesyl thiodiphosphate (FSPP) with the predicted 3D structure of LOS. For clarity, structures are focused on the active site of both enzymes. (A) Amino acid sequence alignment of LOS with SS proteins focusing on the regions around the residues analyzed in this study. The five LOS residues chosen for mutagenesis and the corresponding residues in the SS proteins are shown in red. LOS, lycopaoctaene synthase; LSS, *B. braunii* L race SS; BSS, *B. braunii* B race SS; *At*SS, *Arabidopsis thaliana* SS; YSS, yeast SS; HSS, human SS. (B) Superposition of HSS (light blue) and LOS (light brown) showing the five amino acids of HSS located on the hydrophobic floor of the two substrate binding sites highlighted in magenta. (C) Superposition of HSS (light blue) and LOS (light brown) showing the five amino acids of LOS located on the hydrophobic floor of two substrate binding sites highlighted in magenta.

substrate pocket hydrophobic floor, and Val289 and Ser276 contributing to the S2 substrate pocket hydrophobic floor (Figure 2C). Replacement of HSS Phe288 with Ala288 in LOS and HSS Tyr276 with Ser276 in LOS appears to enlarge the S1 and S2 substrate binding pockets, respectively, to accommodate the larger GGPP substrate (Figure 2C). We therefore hypothesized LOS Ala288 and Ser276 were key mutations that arose during gene duplication to allow GGPP binding while retaining FPP binding. Thus, Ala288 and Ser276 plus the three other residues, Thr65, Met180, and Val289, were chosen for mutational studies to decipher the roles of these amino acids in substrate binding and product specificity.

Characterization of LOS Mutants *in Vitro*. In order to determine the roles of LOS Thr65, Met180, Ser276, Ala288, and Val289 in substrate binding and product formation, these amino acids were mutated to the corresponding HSS residues individually and in combinations (Table 1). The mutated

Table 1. List of Lycopaoctaene Synthase (LOS) Mutants Characterized in This Study

mutant name	mutation
M1	T65V
M2	M180L
M3	S276Y
M4	A288F
M5	V289C
M6	T65V M180L
M7	T65V A288F
M8	V289C S276Y
M9	S276Y A288F
M10	T65V M180L A288F
M11	T65V M180L S276Y A288F
M12	T65V M180L S276Y A288F V289C

proteins were purified, enzyme activity characterized in a mixed substrate assay (Figure 3A) containing equimolar ^{3}H-FPP and ^{3}H-GGPP, and the enzymatic activity quantified based on ^{3}H incorporation into the squalene, $C_{35}H_{58}$, and lycopaoctaene products (Figure 3B). The FPP/GGPP mixed substrate assay was chosen over the FPP/PPP or GGPP/PPP mixed substrate assays because the FPP/GGPP assay is more robust in terms of product formation.[12]

For the M1 to M5 single amino acid mutations the results indicated M1, M2, and M5 retained the ability to produce lycopaoctaene, whereas replacement of Ser276 and Ala288 with the larger aromatic amino acids Tyr and Phe in M3 and M4, respectively, lead to a significant loss of lycopaoctaene production when compared to wild-type (WT; Figure 3B). In the case of $C_{35}H_{58}$ production, all single mutants retained at least WT activity (Figure 3B). Interestingly, the M3 mutant showed a significant increase in $C_{35}H_{58}$ production to 183% of WT LOS (Figure 3B). Except for M3, all single mutants retained at least WT activity levels for squalene production (Figure 3B). The observed activity for M3 and M4 suggests the increased residue size in these mutants blocks GGPP biding in the S1 pocket by the M4 A288F mutation and in the S2 pocket by the M3 S276Y mutation, indicating the importance of LOS Ser276 and Ala288 in GGPP binding. Further support for this is seen by the increased $C_{35}H_{58}$ production in M3 (Figure 3B), suggesting favorable binding of one GGPP in the S1 pocket and one FPP in the S2 pocket. Additionally, the decreased lycopaoctaene production, but no change in squalene and

DOI: 10.1021/acschembio.7b00457
ACS Chem. Biol. 2017, 12, 2408−2416

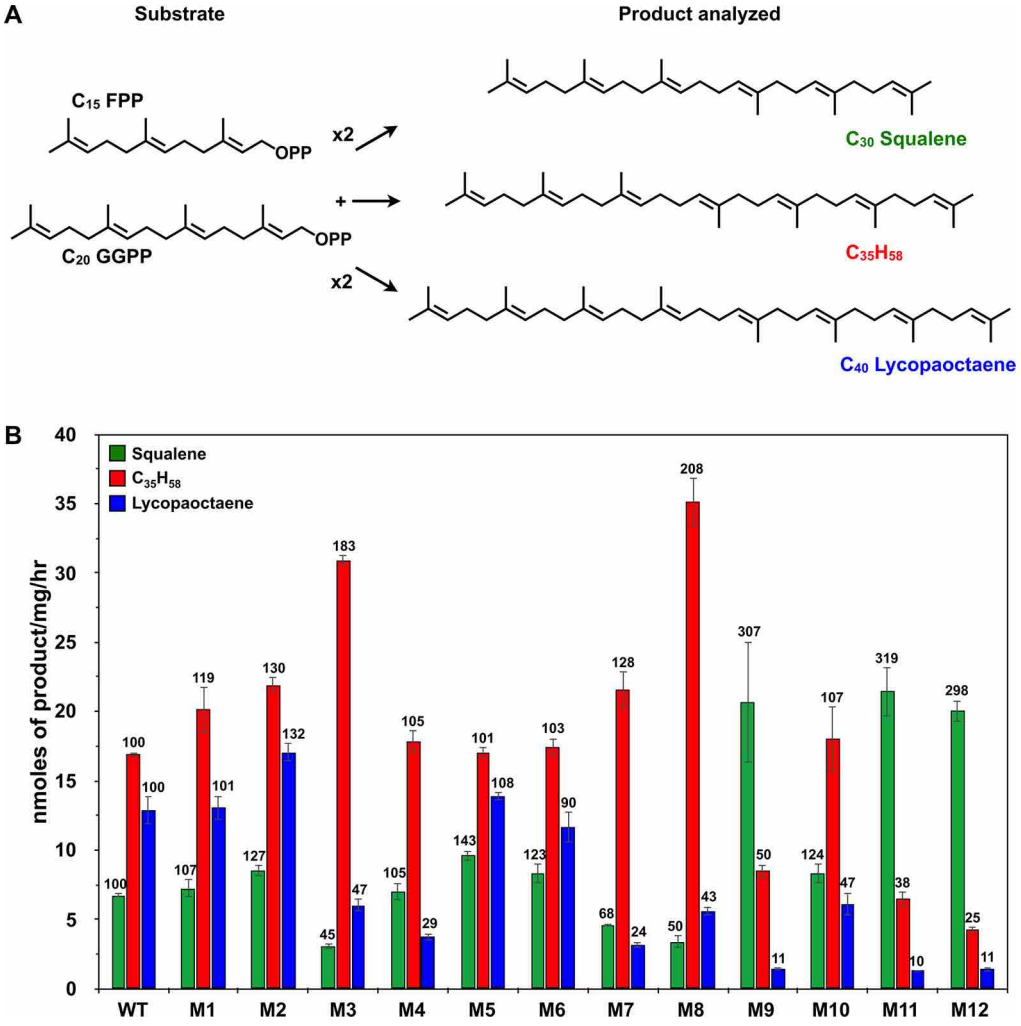

Figure 3. Characterization of LOS mutants *in vitro*. (A) Reaction scheme showing LOS products from the FPP/GGPP mixed substrate assay. (B) Enzyme activities of the LOS mutants in the FPP/GGPP mixed substrate assay showing production of squalene, $C_{35}H_{58}$, and lycopaoctaene. Numbers on top of each bar indicate the activity percentage based on WT LOS activity as 100%. Data shown are from three independent experiments (n = 3). LOS, lycopaoctaene synthase; FPP, farnesyl diphosphate; GGPP, geranylgeranyl diphosphate.

$C_{35}H_{58}$ production in M4 (Figure 3B) suggests limited binding of two GGPP molecules and preferable binding of two FPP molecules, or one FPP in the S1 pocket and one GGPP in the S2 pocket (Figure 3A,B).

Next, the LOS double mutants M6 to M9 (Table 1) were characterized for enzymatic activity using the same mixed substrate assay (Figure 3A). The enzyme activity of M6 is similar to that of WT (Figure 3B). When comparing the M7 double mutant to the parent M4 background, M7 did not show a difference in lycopaoctaene production, but $C_{35}H_{58}$ production was slightly increased and squalene formation was significantly reduced (Figure 3B). For the M8 double mutant, in comparison to the M3 parent background, a small increase in $C_{35}H_{58}$ production was observed, whereas the activities for lycopaoctaene and squalene production remained the same (Figure 3B). Most interestingly, the M9 double mutant, which has both the M3 S276Y and the M4 A288F mutations, showed a drastic reduction in the ability to produce lycopaoctaene and $C_{35}H_{58}$ compared to WT, while the SS activity is substantially increased more than 3-fold over the WT enzyme (Figure 3B). These results for M9 further support our hypothesis that Ser276 and Ala288 are important for controlling LOS substrate binding, and replacing these residues with bulky aromatic amino acids blocks the binding of GGPP in both substrate binding pockets. This is further supported by a previous study where the corresponding Phe288 was shown to be essential in the HSS reaction.[15] The HSS^{F288A} crystal structure showed mutation to the smaller Ala resulted in a deeper cleft in the S1 substrate pocket.[15] Thus, having Ala at position 288 in LOS would expand the S1 substrate pocket to allow GGPP binding. Additionally, Phe288 was proposed to be involved in PSPP diphosphate ionization and orientation.[15] Accordingly, the F288A mutation in HSS significantly reduced enzyme activity to 22.7% of WT activity.[15] Since the WT LOS with Ala288 is fully active, this would suggest additional LOS residues that are different from SS allow for proper PLPP diphosphate orientation and ionization.

Finally, the M10 triple mutant, the M11 quadruple mutant, and the M12 quintuple mutant (Table 1) were analyzed for enzymatic activity using the mixed substrate assay. The M10 mutant showed activity similar to that of the M4 parent background (Figure 3B). For the M11 and M12 mutants, the activities are very similar to each other. But in comparison to the M9 parent background, both M11 and M12 showed a further reduction in $C_{35}H_{58}$ production and no significant change in lycopaoctaene and squalene formation (Figure 3B).

DOI: 10.1021/acschembio.7b00457
ACS Chem. Biol. 2017, 12, 2408−2416

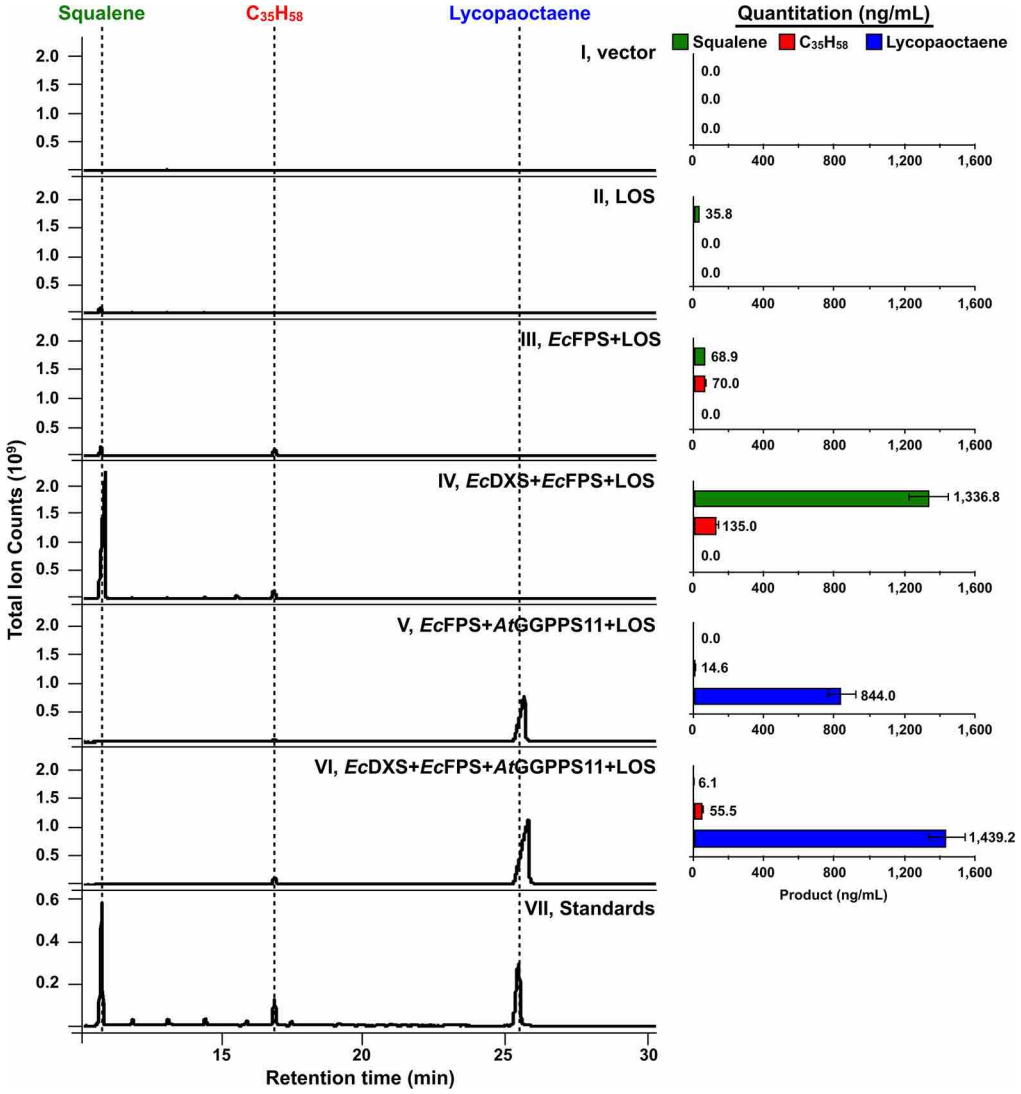

Figure 4. GC-MS profiles and quantitation of *n*-hexane extractable metabolites from *E. coli* cells expressing LOS with MEP pathway gene constructs. (I) Empty vector expression. (II) LOS expression. (III) *Ec*FPS and LOS expression. (IV) *Ec*DXS, *Ec*FPS, and LOS expression. (V) *Ec*FPS, *At*GGPPS11, and LOS expression. (VI) *Ec*DXS, *Ec*FPS, *At*GGPPS11, and LOS expression. (VII) Hydrocarbon standards. Shown to the right of the GC-MS profiles is quantitation of each hydrocarbon based on the GC-MS data and expressed in ng mL^{-1}. The GC-MS data shown are representatives from three independent experiments ($n = 3$), and each experiment was used for quantitation. Numbers shown in the quantitation are the average value for each hydrocarbon. The large amount of squalene and lycopaoctaene in panels IV, V, and VI caused the altered migration of these peaks compared to the standards. MEP, methylerythritol phosphate pathway; LOS, lycopaoctaene synthase; *Ec*FPS, *E. coli* farnesyl diphosphate synthase; *Ec*DXS, *E. coli* deoxyxylulose-5-phosphate synthase; *At*GGPPS11, *Arabidopsis thaliana* geranylgeranyl diphosphate synthase.

These results suggest mutation of the five LOS amino acids studied here to the corresponding HSS residues is sufficient to change LOS substrate binding specificity to mainly FPP binding, and thus product specificity to squalene production (compare WT and M12 in Figure 3B). It should be noted the M12 mutant retained residual activity for lycopaoctaene and $C_{35}H_{58}$ production (Figure 3B), indicating low levels of GGPP binding and suggesting further modification is required in the M12 background to completely abolish GGPP binding (Figure 3B).

Analysis of LOS and LOS Mutants *in Vivo*. To further support the *in vitro* assay data, the activity of WT LOS and the LOS mutants was characterized using *Escherichia coli* as an *in vivo* expression system since the native host, *B. braunii*, cannot be transformed. Like *B. braunii*, *E. coli* utilizes the MEP pathway for isoprenoid biosynthesis.[21] Most importantly, *E. coli* does not naturally produce lycopaoctaene, $C_{35}H_{58}$, or squalene (Figure 4, panel I). Thus, the *E. coli* expression system provides a clean platform on which to characterize LOS and the LOS mutants *in vivo*.

The *in vitro* mixed substrate assays used above for LOS mutant characterization contained equal FPP and GGPP concentrations. Thus, an *E. coli* line generating equal and high amounts of FPP and GGPP is needed for *in vivo* LOS and LOS mutant characterization. However, *E. coli* has limited FPP amounts and even lower GGPP levels.[22] This is consistent with only small amounts of squalene and no $C_{35}H_{58}$ or lycopaoctaene produced from LOS overexpression in *E. coli* (Figure 4, panel II). To overcome this limitation, FPP synthase from *E. coli* (a.k.a. IspA, referred to here as *Ec*FPS) was overexpressed to increase FPP levels. Overexpression of *Ec*FPS with LOS showed squalene production almost doubled, a roughly equal amount of $C_{35}H_{58}$ was detected, and no lycopaoctaene was produced (Figure 4, panel III). This

DOI: 10.1021/acschembio.7b00457
ACS Chem. Biol. 2017, 12, 2408−2416

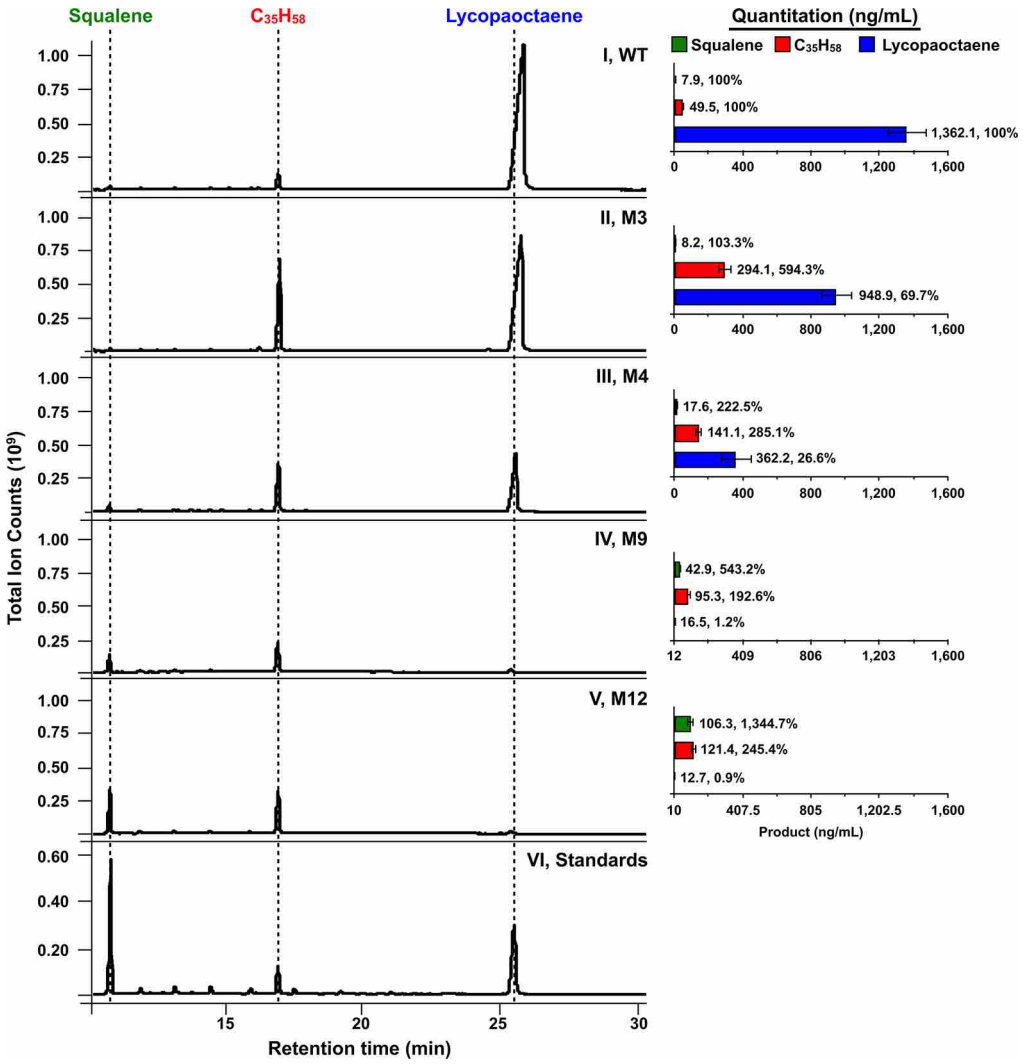

Figure 5. Characterization of LOS mutants *in vivo*. Shown are GC-MS profiles and quantitation of *n*-hexane extractable metabolites from *E. coli* cells expressing WT LOS or select LOS mutants with *Ec*DXS, *Ec*FPS, and *At*GGPPS11. (I) WT LOS expression. (II) LOS M3 mutant expression. (III) LOS M4 mutant expression. (IV) LOS M9 mutant expression. (V) LOS M12 mutant expression. (VI) Hydrocarbon standards. Shown to the right of the GC-MS profiles is quantitation of each hydrocarbon based on the GC-MS data and expressed in ng mL^{-1}. The GC-MS data shown are representatives from three independent experiments ($n = 3$), and each experiment was used for quantitation. Numbers shown in the quantitation are the average value for each hydrocarbon followed by the percent change compared to WT LOS. The large amount of lycopaoctaene in panels I and II caused the altered migration of these peaks compared to the standard. LOS, lycopaoctaene synthase; *Ec*FPS, *E. coli* farnesyl diphosphate synthase; *Ec*DXS, *E. coli* deoxyxylulose-5-phosphate synthase; *At*GGPPS11, *Arabidopsis thaliana* geranylgeranyl diphosphate synthase.

suggests *Ec*FPS overexpression slightly increased intracellular FPP levels, and GGPP levels were high enough to contribute to $C_{35}H_{58}$ production but not high enough for LOS-mediated lycopaoctaene production.

To direct more carbon into the MEP pathway and further boost FPP and GGPP production, deoxyxylulose-5-phosphate synthase from *E. coli* (*Ec*DXS), which catalyzes the first and rate limiting MEP pathway step,[23] was overexpressed with *Ec*FPS and LOS. This expression generated high levels of squalene and increased the amount of $C_{35}H_{58}$ (Figure 4, IV), suggesting a large increase in carbon flux through the MEP pathway to amplify FPP production. However, lycopaoctaene production was still not detected (Figure 4, panel IV), arguing *Ec*DXS overexpression did not increase GGPP pools to a level required for lycopaoctaene biosynthesis.

In order to enhance the GGPP pool, GGPP synthase from *Arabidopsis thaliana* (*At*GGPPS11) was overexpressed along with *Ec*FPS and LOS. Hydrocarbon production analysis in this line showed mainly ample lycopaoctaene production, indicating high levels of GGPP generated by *At*GGPPS11 (Figure 4, panel V). Trace $C_{35}H_{58}$ amounts and no detection of squalene in this line (Figure 4, panel V) may have resulted from an FPP pool reduction by *At*GGPPS11. Additionally, the 2-fold higher LOS affinity for GGPP over FPP[12] likely contributes to preferred lycopaoctaene production when GGPP levels are high. To further boost FPP and GGPP production, we overexpressed *Ec*DXS, *Ec*FPS, and *At*GGPPS11 in one line with LOS. Analysis showed lycopaoctaene production was further enhanced and remained the predominant product, while trace amounts of squalene were detected and $C_{35}H_{58}$ production slightly increased (Figure 4, panel VI). These data suggest both the FPP and GGPP pools increased as a result of *Ec*DXS overexpression in this line.

The sharp change in LOS activity from squalene production (Figure 4, panel IV) to lycopaoctaene production in the presence of *At*GGPPS11 (Figure 4, panel V, VI) suggests the

DOI: 10.1021/acschembio.7b00457
ACS Chem. Biol. 2017, 12, 2408−2416

FPP pools were too low to support LOS squalene production due to FPP conversion to GGPP by *At*GGPPS11. This is supported by LSS mediated squalene production in these engineered *E. coli* lines (Figure S4), which is used as a proxy for FPP levels. Maximal squalene levels were seen when LSS was expressed with *Ec*DXS and *Ec*FPS (Figure S4, panel IV), which was 4.2 times higher than LSS expression alone (Figure S4, panel II). This suggests maximal FPP levels in the *Ec*DXS and *Ec*FPS expressing *E. coli* line. The inclusion of *At*GGPPS11 (with or without *Ec*DXS) reduced squalene production to approximately 1.6 times that of LSS expression alone (Figure S4, panel V, VI), suggesting FPP pools are reduced close to WT *E. coli* levels due to *At*GGPPS11 expression. This lower FPP level in combination with the previously mentioned higher affinity of LOS for GGPP may explain the preference for lycopaoctaene production in the presence of moderate FPP pools and high GGPP pools.

Interestingly, this product specificity of LOS for lycopaoctaene over $C_{35}H_{58}$ and squalene as observed in *E. coli* (Figure 4, panel VI) could mirror hydrocarbon metabolism in *B. braunii* race L. Our past studies have shown that while lycopaoctaene is rapidly converted to lycopadiene, there is no detectable squalene production and low levels of $C_{35}H_{64}$, a reduced product of $C_{35}H_{58}$.[12] This would suggest in the L race LOS has access to high GGPP levels, leading to the product specificity for lycopaoctaene over $C_{35}H_{64}$ or squalene. In *B. braunii* race L, this may come about by metabolic channeling[24] of the MEP pathway toward GGPP, and thus lycopadiene biosynthesis *via* lycopaoctaene production by LOS.

Next, we investigated the *in vivo* activity of several select LOS mutants by coexpression in the *Ec*DXS, *Ec*FPS, and *At*GGPPS11 expressing *E. coli* line, which should have the highest levels of both FPP and GGPP. Although expression of LOS with *Ec*DXS, *Ec*FPS, and *At*GGPPS11 in *E. coli* did not result in a hydrocarbon production profile similar to WT LOS in the *in vitro* mixed substrate assay, expression of the LOS mutants in this *E. coli* line allowed us to generate valuable information as discussed below that further supports the *in vitro* data.

The mutants selected for expression in the *Ec*DXS, *Ec*FPS, and *At*GGPPS11 expressing *E. coli* line were M3, M4, and M9 (Table 1). These mutants are focused on the LOS Ser276 and Ala288 residues, which appear to have the biggest influence on substrate binding and product formation (Figure 3B). Additionally, the M12 mutant (Table 1) was chosen because it contains the full set of five LOS mutations based on the HSS sequence. As previously seen (Figure 4), WT LOS expression in this *E. coli* line predominantly produced lycopaoctaene, a small amount of $C_{35}H_{58}$, and trace amounts of squalene (Figure 5, panel I). Expression of the S276Y M3 mutant showed a reduced level of lycopaoctaene, a large increase in $C_{35}H_{58}$ production, and no change in squalene levels in comparison to WT LOS (Figure 5, panel II). This is similar to what was seen in the M3 *in vitro* assays (Figure 3B). Similarly, in comparison to WT LOS, the A288F M4 mutant *in vivo* showed a reduction in lycopaoctaene production and increased $C_{35}H_{58}$ and squalene production (Figure 5, panel III). These data are also similar to the M4 *in vitro* data, except that M4 *in vitro* had no change in $C_{35}H_{58}$ levels (Figure 3B). For the M9 S276Y/A288F double mutant, its ability to produce lycopaoctaene *in vivo* was drastically reduced, whereas production of $C_{35}H_{58}$ and squalene was increased compared to WT LOS (Figure 5, panel IV). Again, this is similar to what was seen for M9 *in vitro* (Figure 3B); however, the *in vivo* $C_{35}H_{58}$ levels for M9 increased while the *in vitro* $C_{35}H_{58}$ levels decreased compared to WT LOS (Figure 3B). This would indicate some level of GGPP binding by the M9 mutant when high GGPP pools are present *in vivo* (Figure 5, panel IV). As was seen for the *in vitro* assays, the M12 mutant *in vivo* showed a drastic reduction in lycopaoctaene production and a large increase in squalene levels compared to WT LOS (Figure 5, panel V). However, the $C_{35}H_{58}$ levels were higher than WT LOS *in vivo* (Figure 5, panel V), while *in vitro* the $C_{35}H_{58}$ levels decreased for M12 compared to WT LOS (Figure 3). Again, this could be due to high levels of GGPP *in vivo*. As intended, the M12 mutations changed LOS product specificity from lycopaoctaene to squalene both *in vitro* and *in vivo*. Overall, while the absolute changes in product formation for the mutants *in vivo* (Figure 5) do not match that seen for the *in vitro* data (Figure 3), the trends in product formation for the M3, M4, M9, and M12 mutants *in vivo* are consistent with the enzymatic activities observed in the *in vitro* assays.

Structural Insights into the Role of LOS Ser276 and Ala288 in GGPP Binding. The studies presented above indicate LOS residues Ser276 and Ala288 play a key role in substrate binding and product specificity. To gain more insight into the role of these two amino acids in controlling substrate binding, we compared the HSS structure in complex with FSPP to the predicted LOS structure focusing on HSS Tyr276 and Phe288 and LOS Ser276 and Ala288 (Figure 6A). The analysis showed the distances in HSS from the Phe288 benzene ring and the Tyr276 phenol group to the corresponding S1 and S2 FSPP tails are 3.54 and 4.35 Å, respectively (Figure 6A). Given that GGPP is 4.00−4.80 Å longer than FPP, depending on which branch of the terminal isoprene unit is used for measurement, this analysis suggests HSS cannot bind GGPP because the bulky Phe288 in the S1 binding site would clash with GGPP, and taking into account atomic radii and repulsion between atoms Tyr276 in the S2 binding site would interfere with GGPP binding. This notion is further supported by the observed LOS M9 double mutant *in vitro* and *in vivo* enzyme activities, which showed substantial losses of lycopaoctaene and $C_{35}H_{58}$ formation, and a large increase in squalene production as a result of replacing the small Ser276 and Ala288 residues with Tyr and Phe, respectively (Figure 3B and Figure 5, panel IV). Further support of Ser276 and Ala288 controlling GGPP binding in LOS is the 7.85 Å between the Ala288 side chain and the S1 FSPP tail, and the 7.06 Å between the Ser276 hydroxyl group and the S2 FSPP tail (Figure 6A). These distances should provide enough room in the two LOS substrate binding sites to accommodate the longer GGPP hydrophobic tail.

Additional characterization of the two substrate binding sites was conducted by comparing the HSS structure and the predicted LOS structure with the *Staphylococcus aureus* dehydrosqualene synthase (CrtM) structure bound to the GGPP analog geranylgeranyl thiodiphosphate (GGSPP; Figure 6B).[19] CrtM catalyzes an SS-like reaction, except the second reaction step is an NADPH-independent rearrangement of PSPP to produce dehydrosqualene,[19] which contains a *cis* double bond at the linkage between the two FPP molecules (Figure S5). Except for the NADPH binding residues, CrtM shares sequence similarity with the conserved SS domains,[25] and the substrate binding sites in CrtM and HSS are structurally homologous.[15,19] Although the natural substrate of CrtM is FPP, CrtM can also utilize GGPP to produce a C_{35} version of dehydrosqualene in the presence of elevated GGPP

DOI: 10.1021/acschembio.7b00457
ACS Chem. Biol. 2017, 12, 2408−2416

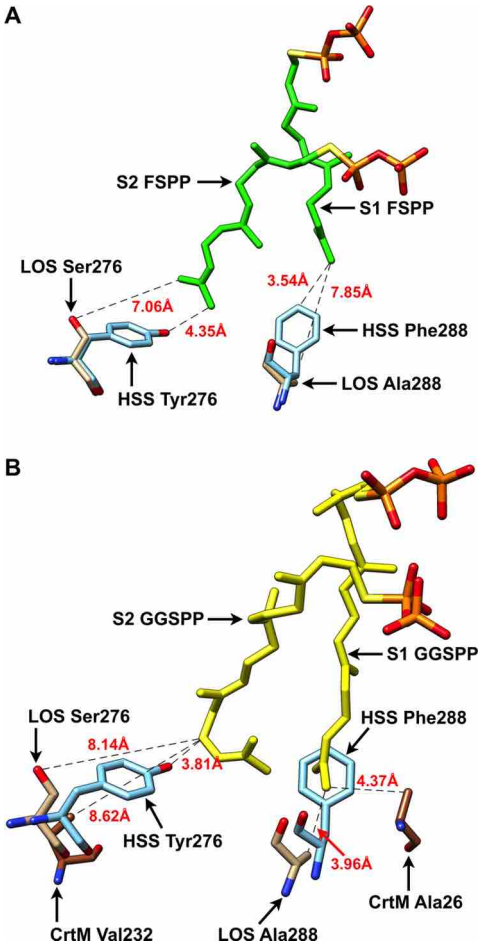

Figure 6. Position comparison of the key residues controlling substrate binding from HSS, LOS, and CrtM in relation to the FSPP (A) and GGSPP (B) substrate analogs. (A) Superposition of the HSS crystal structure bound to two FSPP molecules and the predicted LOS 3D-structure. (B) Superposition of the CrtM crystal structure bound to two GGSPP molecules, the HSS crystal structure (FSPP removed), and the predicted LOS 3D structure. HSS, human squalene synthase; LOS, lycopaoctaene synthase; FSPP, farnesyl thiodiphosphate; GGSPP, geranylgeranyl thiodiphosphate.

levels.[26] This is presumably due to GGPP binding in the S2 site and FPP in the S1 site.[19] This is supported by mutation of the bulky CrtM Phe26 residue to Ala and the structure of the CrtM^{F26A} protein, which showed binding of the longer GGPP substrate at the S1 site and production of a C_{40} version of dehydrosqualene.[19,25]

The structural comparison of HSS, LOS, and CrtM^{F26A} complexed with GGSPP reveals additional insights into substrate binding. The analysis showed HSS Phe288 would clash with the GGSPP hydrophobic tail in the S1 substrate binding site (Figure 6B). In contrast, the distances from LOS Ala288 and CrtM Ala26 to the GGSPP tail are 3.96 and 4.37 Å, respectively, and would provide enough room for GGPP binding in both enzymes (Figure 6B). In the S2 substrate binding site, the GGSPP tail, especially the terminal isoprene unit, is in a bent conformation (Figure 6B). The closest distance between the HSS Tyr276 hydroxyl group and GGSPP is to the first carbon of the terminal GGSPP isoprene unit at 3.81 Å (Figure 6B), a distance likely not large enough to fit GGPP into the S2 binding even assuming GGPP adopts the bent configuration (Figure 6B). This is supported by our previous finding that typical SS enzymes cannot utilize GGPP.[12] Additionally, mutation of the small LOS Ser276 to the bulky Tyr (M3 mutant) resulted in a substantial loss of lycopaoctaene formation (Figure 3B), corroborating limited S2 site binding of GGPP due to interference from the Tyr. This interference could be further aggravated if the S2 GGPP adopts a more linear conformation. The distance between the LOS Ser276 hydroxyl group and the nearest carbon of GGSPP is 8.14 Å for the current side chain rotamer (Figure 6B), indicating that even with GGPP in a linear conformation there is sufficient room to accommodate GGPP in the S2 substrate binding site. This assumption is further supported by the 8.62 Å distance between GGSPP and CrtM Val232 in the S2 substrate binding site (Figure 6B).

Altogether, our data support the hypothesis that small structural changes due to the replacement of the bulky Tyr276 and Phe288 residues with Ser276 and Ala288, respectively, in the substrate binding sites of an ancestral *B. braunii* race L SS enzyme resulted in the neofunctionalized LOS enzyme with the ability to utilize GGPP to produce the tetraterpenoid hydrocarbon lycopaoctaene. Although LOS evolved larger substrate binding pockets to accept GGPP, these larger substrate pockets do not prevent binding of the smaller FPP substrate, thus leading to the substrate promiscuity observed for this enzyme.

■ ASSOCIATED CONTENT

Supporting Information

The Supporting Information is available free of charge on the ACS Publications website at DOI: 10.1021/acschembio.7b00457.

Supporting Figures S1−S5 and Methods (PDF)

■ AUTHOR INFORMATION

Corresponding Author

*E-mail: tpd8@tamu.edu.

ORCID

Timothy P. Devarenne: 0000-0001-6032-8049

Present Address

§School of Chemistry and Biochemistry, Georgia Institute of Technology, Atlanta GA 30332, USA

Notes

The authors declare no competing financial interest.

■ ACKNOWLEDGMENTS

This work was supported by grant NSF-EFRI-PSBR #1240478 to T.P.D.

■ REFERENCES

(1) Vranova, E., Coman, D., and Gruissem, W. (2013) Network analysis of the MVA and MEP pathways for isoprenoid synthesis. *Annu. Rev. Plant Biol. 64*, 665−700.

(2) Kirby, J., and Keasling, J. D. (2009) Biosynthesis of plant isoprenoids: perspectives for microbial engineering. *Annu. Rev. Plant Biol. 60*, 335−355.

(3) Beller, H. R., Lee, T. S., and Katz, L. (2015) Natural products as biofuels and bio-based chemicals: fatty acids and isoprenoids. *Nat. Prod. Rep. 32*, 1508−1526.

(4) Lee, S. Y., Kim, H. M., and Cheon, S. (2015) Metabolic engineering for the production of hydrocarbon fuels. *Curr. Opin. Biotechnol. 33*, 15−22.

DOI: 10.1021/acschembio.7b00457
ACS Chem. Biol. 2017, 12, 2408−2416

(5) Gupta, P., and Phulara, S. C. (2015) Metabolic engineering for isoprenoid-based biofuel production. *J. Appl. Microbiol. 119*, 605−619.
(6) Metzger, P., and Largeau, C. (2005) *Botryococcus braunii*: a rich source for hydrocarbons and related ether lipids. *Appl. Microbiol. Biotechnol. 66*, 486−496.
(7) Behar, F., Derenne, S., and Largeau, C. (1995) Closed pyrolyses of the isoprenoid algaenan of *Botryococcus-braunii*, L race - Geochemical implications for derived kerogens. *Geochim. Cosmochim. Acta 59*, 2983−2997.
(8) Hillen, L. W., Pollard, G., Wake, L. V., and White, N. (1982) Hydrocracking of the oils of *Botryococcus braunii* to transport fuels. *Biotechnol. Bioeng. 24*, 193−205.
(9) Banerjee, A., Sharma, R., Chisti, Y., and Banerjee, U. C. (2002) *Botryococcus braunii*: a renewable source of hydrocarbons and other chemicals. *Crit. Rev. Biotechnol. 22*, 245−279.
(10) Metzger, P., and Casadevall, E. (1987) Lycopadiene, a tetraterpenoid hydrocarbon from new strains of the green alga *Botryococcus braunii*. *Tetrahedron Lett. 28*, 3931−3934.
(11) Metzger, P., Allard, B., Casadevall, E., Berkaloff, C., and Coute, A. (1990) Structure and chemistry of a new chemical race of *Botryococcus braunii* (Chlorophyceae) that produces lycopadiene a tetraterpenoid hydrocarbon. *J. Phycol. 26*, 258−266.
(12) Thapa, H. R., Naik, M. T., Okada, S., Takada, K., Molnar, I., Xu, Y., and Devarenne, T. P. (2016) A squalene synthase-like enzyme initiates production of tetraterpenoid hydrocarbons in *Botryococcus braunii* race L. *Nat. Commun. 7*, 11198.
(13) Jarstfer, M. B., Blagg, B. S. J., Rogers, D. H., and Poulter, C. D. (1996) Biosynthesis of squalene. Evidence for a tertiary cyclopropylcarbinyl cationic intermediate in the rearrangement of presqualene diphosphate to squalene. *J. Am. Chem. Soc. 118*, 13089−13090.
(14) Liu, C. I., Jeng, W. Y., Chang, W. J., Ko, T. P., and Wang, A. H. (2012) Binding modes of zaragozic acid A to human squalene synthase and staphylococcal dehydrosqualene synthase. *J. Biol. Chem. 287*, 18750−18757.
(15) Liu, C. I., Jeng, W. Y., Chang, W. J., Shih, M. F., Ko, T. P., and Wang, A. H. (2014) Structural insights into the catalytic mechanism of human squalene synthase. *Acta Crystallogr., Sect. D: Biol. Crystallogr. 70*, 231−241.
(16) Pandit, J., Danley, D. E., Schulte, G. K., Mazzalupo, S., Pauly, T. A., Hayward, C. M., Hamanaka, E. S., Thompson, J. F., and Harwood, H. J., Jr. (2000) Crystal structure of human squalene synthase. A key enzyme in cholesterol biosynthesis. *J. Biol. Chem. 275*, 30610−30617.
(17) Gu, P., Ishii, Y., Spencer, T. A., and Shechter, I. (1998) Function-structure studies and identification of three enzyme domains involved in the catalytic activity in rat hepatic squalene synthase. *J. Biol. Chem. 273*, 12515−12525.
(18) Robinson, G. W., Tsay, Y. H., Kienzle, B. K., Smith-Monroy, C. A., and Bishop, R. W. (1993) Conservation between human and fungal squalene synthetases: similarities in structure, function, and regulation. *Mol. Cell. Biol. 13*, 2706−2717.
(19) Lin, F. Y., Liu, C. I., Liu, Y. L., Zhang, Y., Wang, K., Jeng, W. Y., Ko, T. P., Cao, R., Wang, A. H., and Oldfield, E. (2010) Mechanism of action and inhibition of dehydrosqualene synthase. *Proc. Natl. Acad. Sci. U. S. A. 107*, 21337−21342.
(20) Shang, N., Li, Q., Ko, T. P., Chan, H. C., Li, J., Zheng, Y., Huang, C. H., Ren, F., Chen, C. C., Zhu, Z., Galizzi, M., Li, Z. H., Rodrigues-Poveda, C. A., Gonzalez-Pacanowska, D., Veiga-Santos, P., de Carvalho, T. M., de Souza, W., Urbina, J. A., Wang, A. H., Docampo, R., Li, K., Liu, Y. L., Oldfield, E., and Guo, R. T. (2014) Squalene synthase as a target for Chagas disease therapeutics. *PLoS Pathog. 10*, e1004114.
(21) Rohmer, M., Knani, M., Simonin, P., Sutter, B., and Sahm, H. (1993) Isoprenoid biosynthesis in bacteria: a novel pathway for the early steps leading to isopentenyl diphosphate. *Biochem. J. 295*, 517−524.
(22) Reiling, K. K., Yoshikuni, Y., Martin, V. J., Newman, J., Bohlmann, J., and Keasling, J. D. (2004) Mono and diterpene production in *Escherichia coli*. *Biotechnol. Bioeng. 87*, 200−212.
(23) Zhao, L., Chang, W. C., Xiao, Y., Liu, H. W., and Liu, P. (2013) Methylerythritol phosphate pathway of isoprenoid biosynthesis. *Annu. Rev. Biochem. 82*, 497−530.
(24) Jorgensen, K., Rasmussen, A. V., Morant, M., Nielsen, A. H., Bjarnholt, N., Zagrobelny, M., Bak, S., and Møller, B. L. (2005) Metabolon formation and metabolic channeling in the biosynthesis of plant natural products. *Curr. Opin. Plant Biol. 8*, 280−291.
(25) Umeno, D., and Arnold, F. H. (2004) Evolution of a pathway to novel long-chain carotenoids. *J. Bacteriol. 186*, 1531−1536.
(26) Umeno, D., and Arnold, F. H. (2003) A C_{35} carotenoid biosynthetic pathway. *Appl. Environ. Microbiol. 69*, 3573−3579.

DOI: 10.1021/acschembio.7b00457
ACS Chem. Biol. 2017, 12, 2408−2416

Supporting Information for:

Substrate and product specificity for a tetraterpenoid synthase from the green microalga *Botryococcus braunii* race L

Hem Raj Thapa,[†] Su Tang,[†] James C. Sacchettini,[†,‡] Timothy P. Devarenne*,[†]

[†]Department of Biochemistry & Biophysics, Texas A&M University, College Station TX 77843, USA

[‡]Department of Chemistry, Texas A&M University, College Station TX 77843, USA

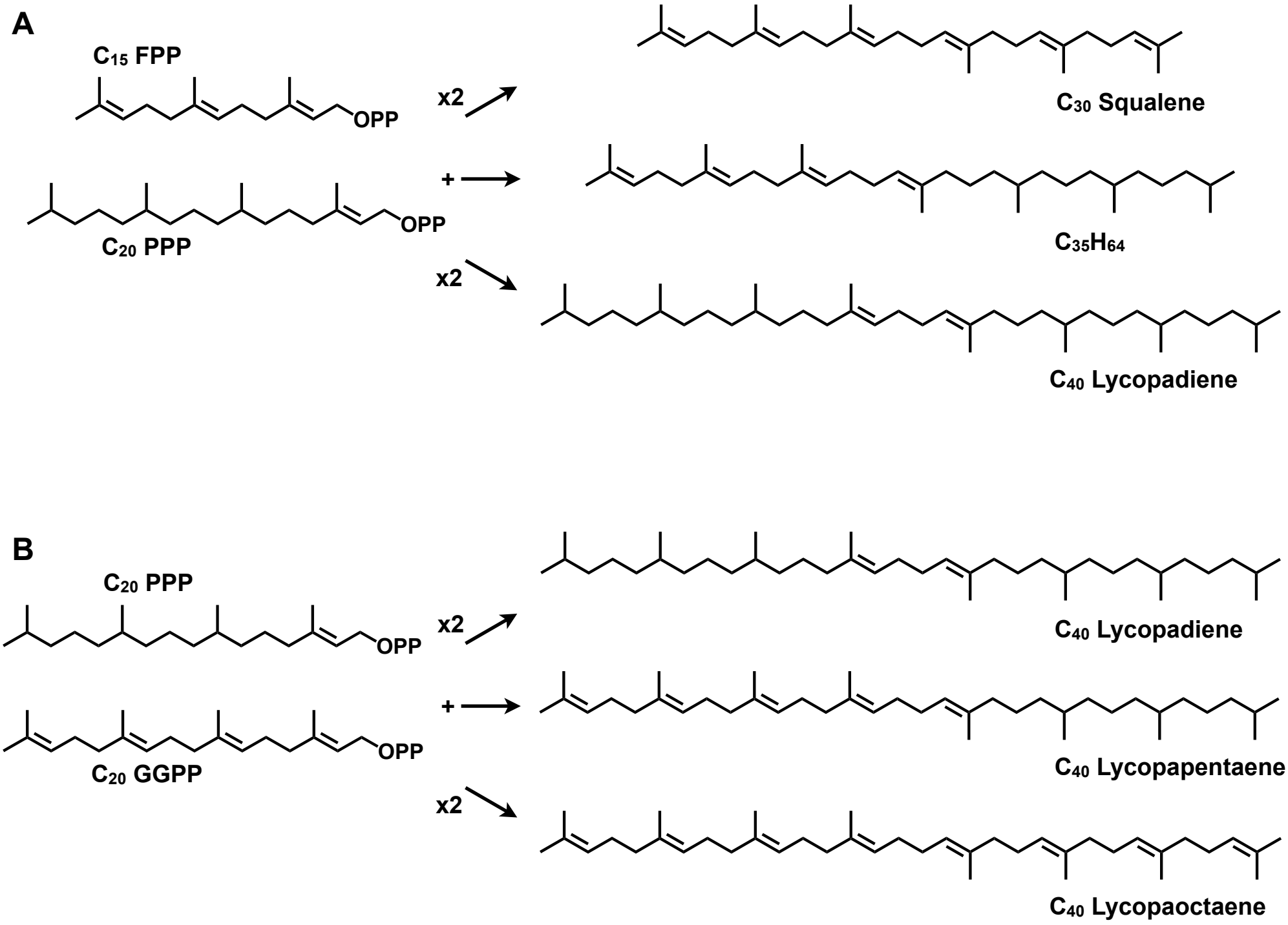

Figure S1. LOS reactions products when incubated with equimolar amounts of (A) FPP and PPP, or (B) GGPP and PPP.

```
                                                                  FLAP
LOS       ----MKYTDFLAHPDEIIPTIRMMYADYRLK----NMEIKDPSVRFCYNMLNRVSRSFAM 52
LSS       MG---KLQEVLKHPDELVPLMQMLVSDYYT-----KIVPRDPGLGFCYRMLNKVSRSFAI 52
BSS       MGMLRWGVESLQNPDELIPVLRMIYADKFG-----KIKPKDEDRGFCYEILNLVSRSFAI 55
AtSS      MG---SLGTMLRYPDDIYPLLKMKRAIEKAE----KQIPPEPHWGFCYSMLHKVSRSFSL 53
YSS       MG---KLLQLALHPVEMKAALKLKFCRTP--LFSIYDQSTSPYLLHCFELLNLTSRSFAA 55
HSS       ----MEFVKCLGHPEEFYNLVRFRIGGKRKVMPKMDQDSLSSSLKTCYKYLNQTSRSFAA 56
                     * ::   :::                    .     *:  *: .****:
                Domain I          Domain II
LOS       VIQQLPVELRDATCVFYLILRALDTVEDDMAIPKEVKIPMLRTFHEHLSDRSWKIKCGY- 111
LSS       VIQQLPELLRDPICVFYLVLRALDTVEDDMALPNDIKLPLLRAFHKKIYDRKWSMKCGY- 111
BSS       VIQQLPAQLRDPVCIFYLVLRALDTVEDDMKIAATTKIPLLRDFYEKISDRSFRMTAGDQ 115
AtSS      VIQQLNTELRNAVCVFYLVLRALDTVEDDTSIPTDEKVPILIAFHRHIYDTDWHYSCGT- 112
YSS       VIRELHPELRNCVTLFYLILRALDTIEDDMSIEHDLKIDLLRHFHEKLLLTKWSFDGNAP 115
HSS       VIQALDGEMRNAVCIFYLVLRALDTLEDDMTISVEKKVPLLHNFHSFLYQPDWRFMESK- 115
          **: *   :*:   :***:******:***  :    *: :*  *:  :   .:    .

LOS       -GPYVDLMDNYPLVTDVYLRFDEGTKAVIKDITRRMGNGMADFIDLD-----EVLTIPQY 165
LSS       -GPYVQLMEEYPMVTGVFLKLDPGPREVITEICRKMGAGMAEFIPKE-----VL-TVKDY 164
BSS       -KDYIRLLDQYPKVTSVFLKLTPREQEIIADITKRMGNGMADFVHKG-----VPDTVGDY 169
AtSS      -KEYKILMDQFHHVSAAFLELEKGYQEAIEEITRRMGAGMAKFICQE-----VE-TVDDY 165
YSS       DVKDRAVLTDFESILIEFHKLKPEYQEVIKEITEKMGNGMADYILDENYNLNGLQTVHDY 175
HSS       -EKDRQVLEDFPTISLEFRNLAEKYQTVIADICRRMGIGMAEFLDKH-----VT-SEQEW 168
               :: ::  :   : .:    :  * :* .:** ***.::           :  ::
               Domain III                          Domain IV
LOS       DLYCHYVAGLCGIGMCKLFVDSGLEKEDLVAEEDLANQMGLFLQKNNIVRDYLEDINELP 225
LSS       DQYCHYAAGLVGEGLSKLAVGSGLENPVLLQKEDLSNHMGLFLQKTNIVRDYLEDINEEP 224
BSS       DLYCHYVAGVVGLGLSQLFVASGLQSPSLTRSEDLSNHMGLFLQKTNIIRDYFEDINELP 229
AtSS      DEYCHYVAGLVGLGLSKLFLAAGSEVLT-PDWEAISNSMGLFLQKTNIIRDYLEDINEIP 224
YSS       DVYCHYVAGLVGDGLTRLIVIAKFANESLYSNEQLYESMGLFLQKTNIIRDYNEDLV--- 232
HSS       DKYCHYVAGLVGIGLSRLFSASEFEDPLVGEDTERANSMGLFLQKTNIIRDYLEDQQ--- 225
          * ****.**: * *: :*   :              : *******.**:*** **

LOS       APRMFWPKEIWGNYAKQLDEFKDPKNLDKAMLCLNHMVTDALRHCEVGLRSLSLLHNPNI 285
LSS       APRMFWPKEIWGKYTKDLADFKDPANEKGAVQCLNHMVTDALRHGEHALKYMALLRDPQY 284
BSS       APRMFWPREIWGKYANNLAEFKDPANKAAAMCCLNEMVTDALRHAVYCLQYMSMIEDPQI 289
```

```
AtSS      KSRMFWPREIWGKYADKLEDLKYEENTNKSVQCLNEMVTNALMHIEDCLKYMVSLRDPSI 284
YSS       DGRSFWPKEIWSQYAPQLKDFMKPENEQLGLDCINHLVLNALSHVIDVLTYLASIHEQST 292
HSS       GGREFWPQEVWSRYVKKLGDFAKPENIDLAVQCLNELITNALHHIPDVITYLSRLRNQSV 285
            * ***:*:*..*. .* ::    *   .: *:*.:: :** *    :  :  :.: .
               Domain V                    JK loop
LOS       LRAVLIPQVMGVRTLTLVYNNPEVFRG---VVKMRRGETAKIFVTTTSKLSFFRTYLQFA 342
LSS       FNFCAIPQVMAFGTLSLCYNNPQVFKG---VVKLRKGESAKLMTTVKSMPALYRTFLRMA 341
BSS       FNFCAIPQTMAFGTLSLCYNNYTIFTGPKAAVKLRRGTTAKLMYTSNNMFAMYRHFLNFA 349
AtSS      FRFCAIPQIMAIGTLALCYNNEQVFRG---VVKLRRGLTAKVIDRTKTMADVYGAFYDFS 341
YSS       FQFCAIPQVMAIATLALVFNNREVLHG---NVKIRKGTTCYLILKSRTLRGCVEIFDYYL 349
HSS       FNFCAIPQVMAIATLAACYNNQQVFKG---AVKIRKGQAVTLMMDATNMPAVKAIIYQYM 342
          :.   *** *.. **:  :**  :: *    **:*:* :  ::    .

LOS       NEMEQKCLTEAKNDPMVALTLKRVQGVQAACRAA----------------IVKAEIAEG 385
LSS       DDMVARCKGEARQDPNVATTLKRLQAIQAVCKTG----------------LRSSIKSRK 384
BSS       EKLEVRCNTETSEDPSVTTTLEHLHKIKAACKAG----------------LARTKDDTF 392
AtSS      CMLKTK---VDKNDPNASKTLNRLEAVQKLCRDA----------------GVLQNRKSY 381
YSS       RDIKSK---LAVQDPNFLKLNIQISKIEQFMEEMYQDKLPPNVKPNETPIFLKVKERSRY 406
HSS       EEIYHR---IPDSDPSSSKTRQIISTIRTQNLPN----------------CQLISRSHY 382
            :  :      .**        :  :.

LOS       A--KGPSTA-------MVLAG-AL-LIAALAYFAYVYSAGGTS-LKALPLFG-------V 426
LSS       KQAATPLSD-------DFISKLVL-V-LGLGYCVYAFNLLPLL--------------WKS 421
BSS       D---------------ELRSRLLA-LTGGSFYLAWTYNFLDLRGPGDLPTFLSVTQHWWS 436
AtSS      VNDKGQPNS-------VFIIMVVILLAIVFAYLRAN---------------------- 410
YSS       DDELVPTQQEEEYKFNMVLSIILS-VLLGFY---YIYTLHRA---------------- 444
HSS       -------SP-------IYLSFVML-----LAALSWQYLTTLSQVTED---YVQTGEH--- 417


LOS       VIILAIG--LF---GRNLALKTV--------------------------     444
LSS       ----------ALIPGPPPPALTSSLGLPHQIIAVFCVLTAGYQVFLRGGLA    462
BSS       ILIFLISIAVFFIPSRPSPRPTLSA------------------------     461
AtSS      ---------------------------------------------------    410
YSS       ---------------------------------------------------    444
HSS       ---------------------------------------------------    417
```

Figure S2. Amino acid sequence alignment of LOS with squalene synthase (SS) proteins from different organisms using Clustal Omega. Conserved domains and regions found in a typical squalene synthases are highlighted indicated above the sequence. The FPP/PSSPP diphosphate binding binding motifs are shown in blue, NADPH binding residues are highlighted in green, and the residues of LOS chosen for mutagenesis and the corresponding residues in the SS proteins are shown in red. Transmembrane domain predicted by TMpred for each protein are underlined. LOS, lycopaoctaene synthase (AC# KT388101); LSS, SS from *Botryococcus braunii* race L (AC# KT388100); BSS, SS from *Botryococcus braunii* race B (AC# AH009227); *At*SS, SS from *Arabidopsis thaliana* (AC# D29017.1); YSS, SS from *Saccharomyces cerevisae* (AC# M63979.1); and HSS, Human SS (AC# Q6IAX1).

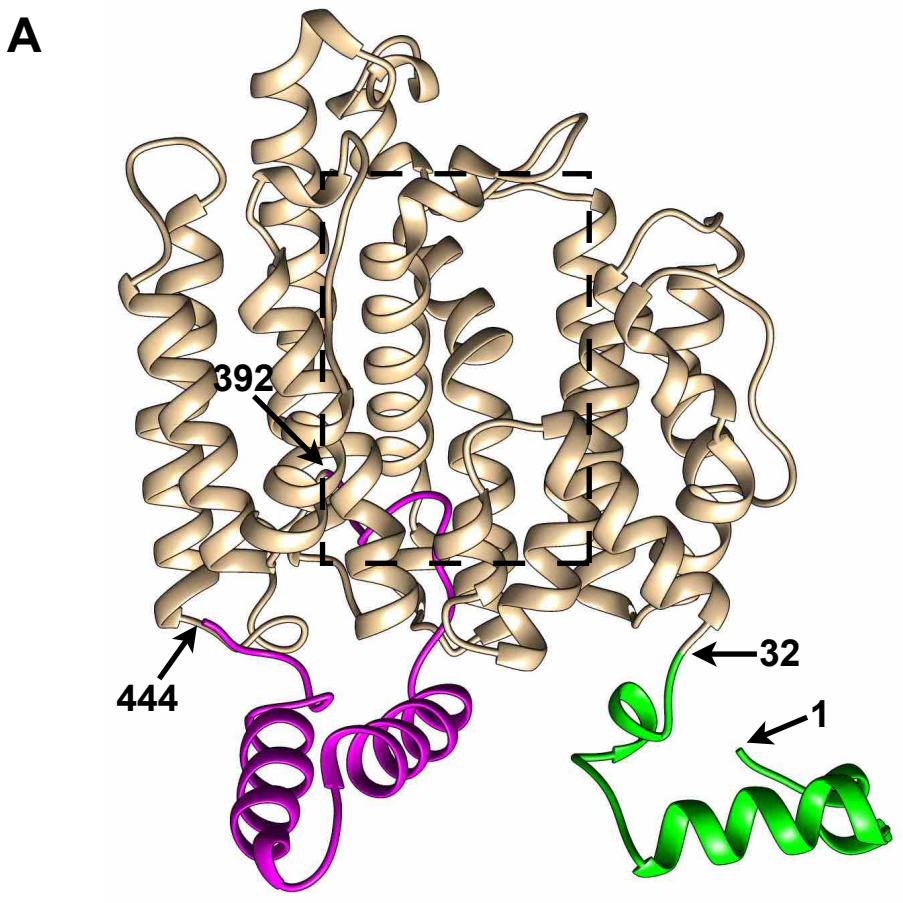

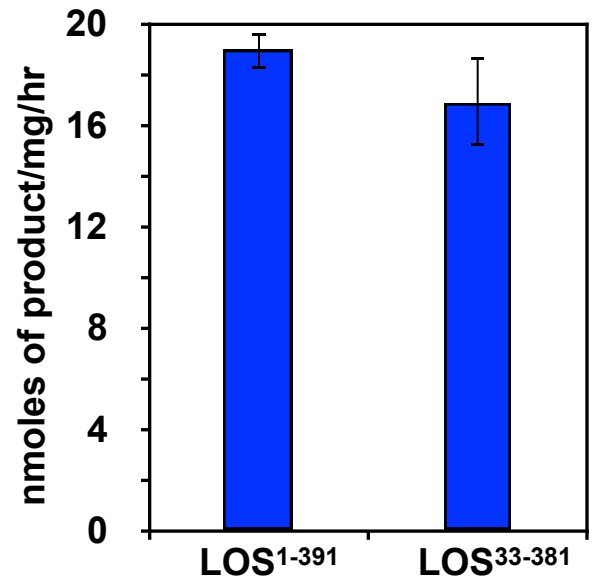

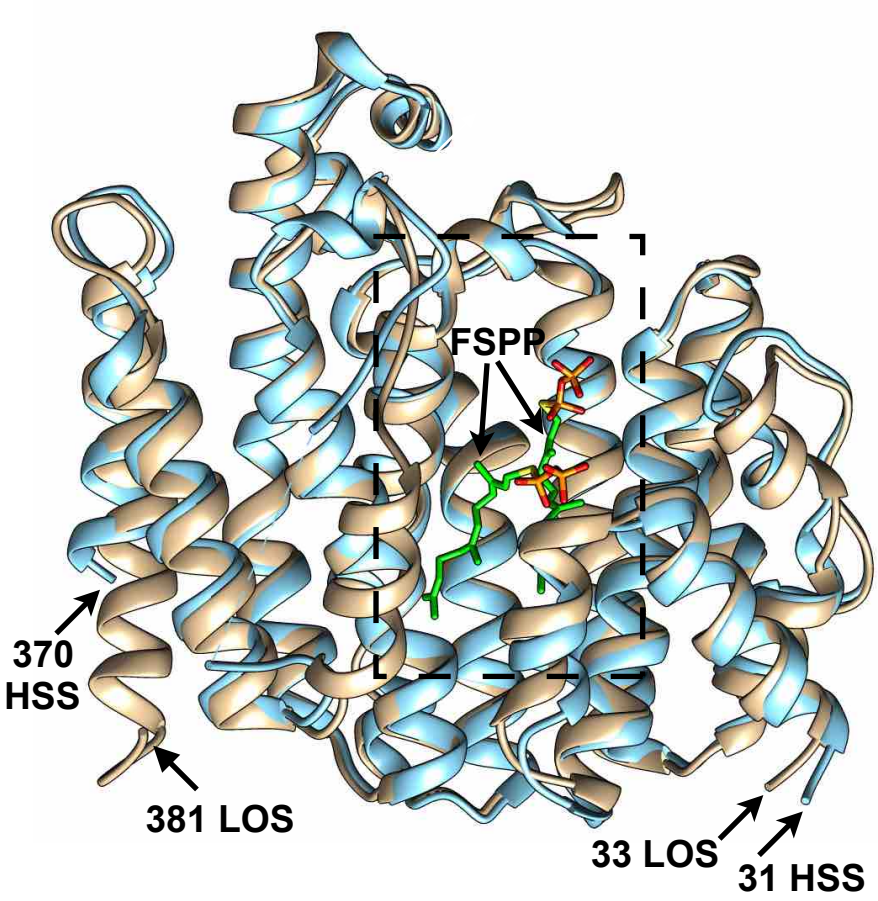

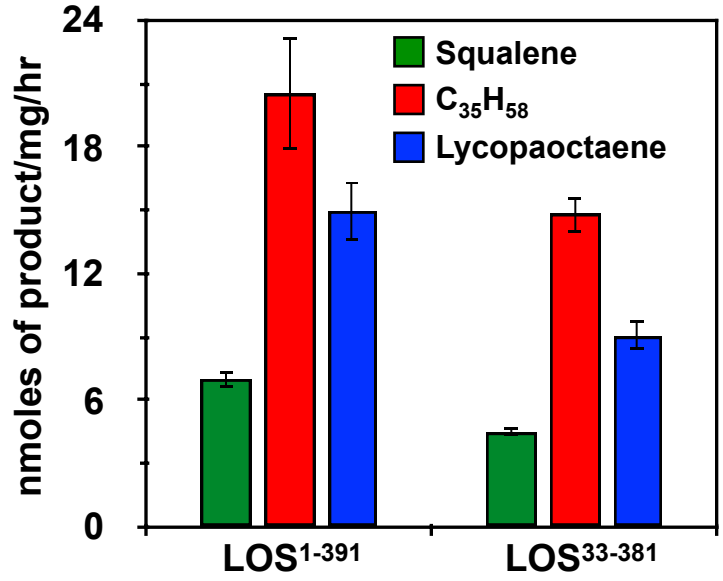

Figure S3. 3D-Structures of lycopaoctaene synthase (LOS) and human squalene synthase (HSS). (A) A model of the LOS structure as predicted by the I-TASSER program. The N-terminal flexible region is shown in green and a double pass transmembrane domain predicted by TMPred software is shown in magenta. (B) LOS enzyme assay for lycopaoctaene production using LOS^{1-391} and LOS^{33-381} with geranylgeranyl diphosphate (GGPP) given as a substrate. (C) Comparison of the crystal structure of HSS^{31-370} (light blue) bound to two molecules of farnesylthiol diphosphate (FSPP) and a computationally truncated model of LOS^{33-381} (light brown). (D) Enzyme activities of LOS^{1-391} and LOS^{33-381} in the FPP/GGPP mixed substrate assay showing production of squalene, $C_{35}H_{58}$, and lycopaoctaene.

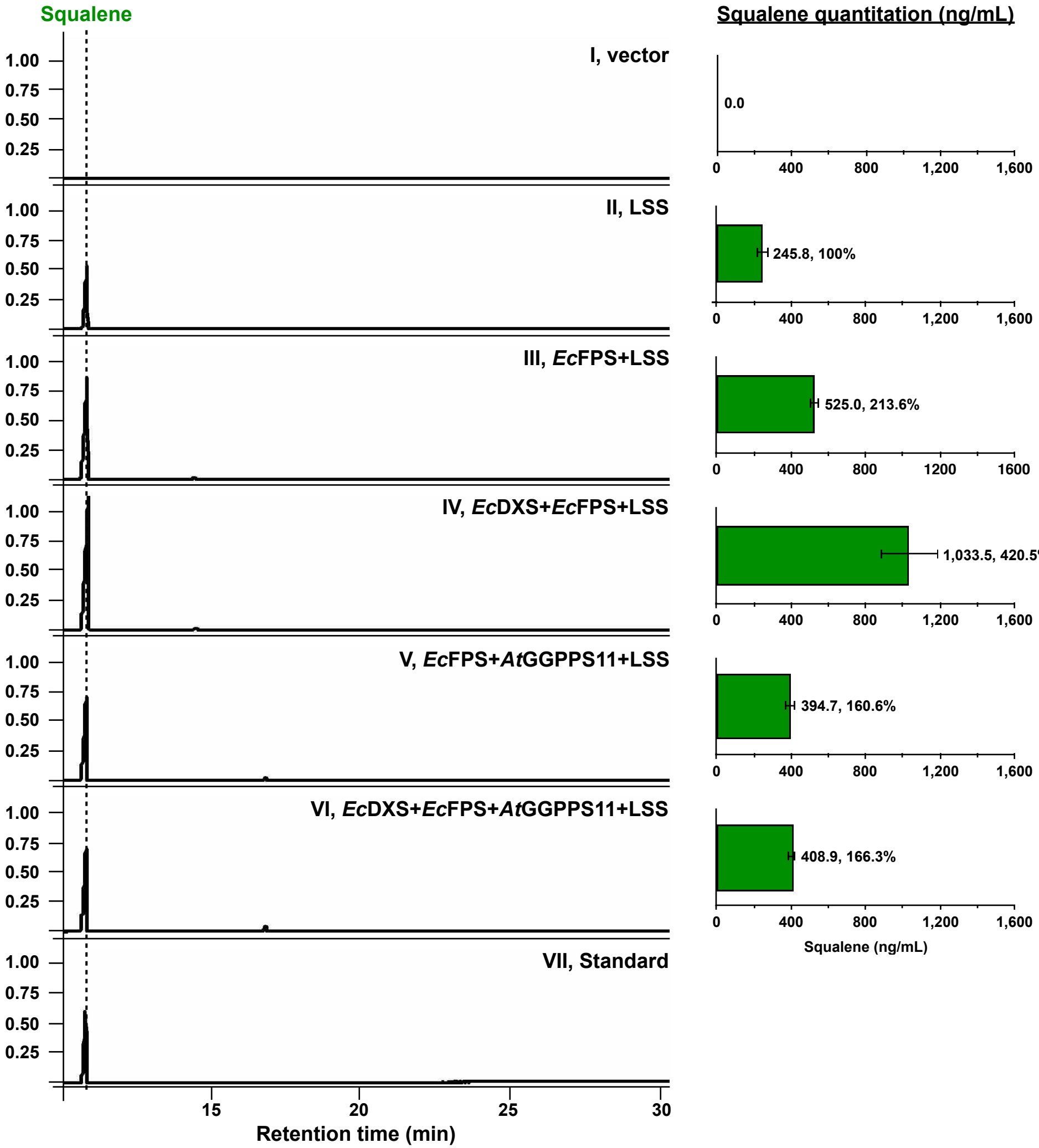

Figure S4. GC-MS profiles and quantitation of *n*-hexane extractable metabolites from *E. coli* cells expressing LSS with MEP pathway gene constructs. (I) Empty vector expression. (II) LSS expression. (III) *Ec*FPS and LSS expression. (IV) *Ec*DXS, *Ec*FPS, and LSS expression. **(**V) *Ec*FPS, *At*GGPPS11, and LSS expression. (VI) *Ec*DXS, *Ec*FPS, *At*GGPPS11, and LSS expression. (VII) Squalene standard. Shown to the right of the GC-MS profiles is quantitation of squalene based on the GC-MS data and expressed in ng/mL. The GC-MS data shown are representatives from three independent experiments (n = 3) and each experiment was used for quantitation. Numbers shown in the quantitation are the average value for squalene.

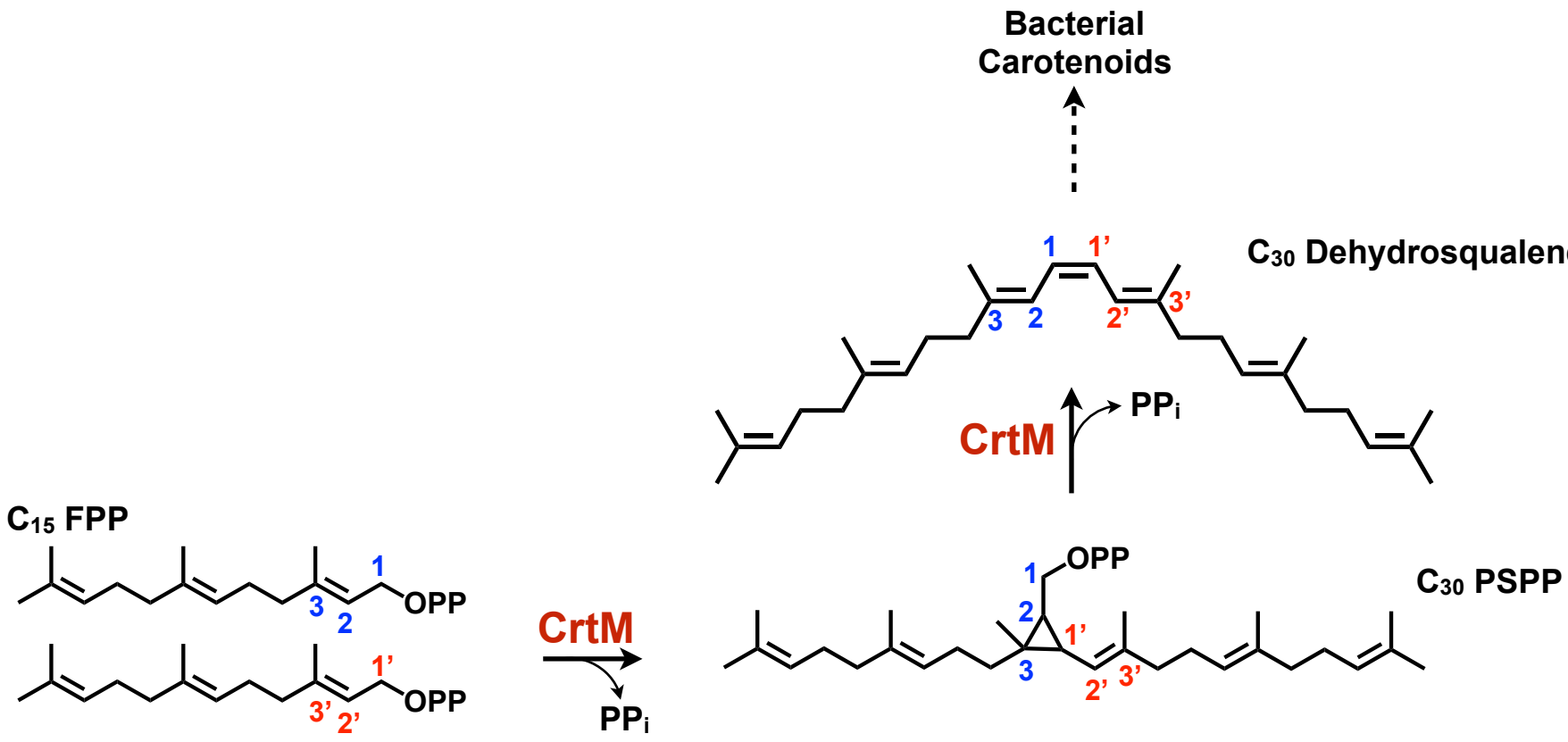

Figure S5. The two step reaction carried out by *S. aureus* CrtM to produce dehydrosqualene.

METHODS

Reagents. Radiolabeled substrates [1-^{3}H]-FPP (specific activity, 18.2 Ci mmol^{-1}) and [1-^{3}H]-GGPP (specific activity, 20.0 Ci mmol^{-1}) were purchased from PerkinElmer, and non-labeled FPP and GGPP were purchased from Sigma. All other chemicals were purchased from VWR unless otherwise noted.

Protein sequences for amino acid comparison. The following proteins were used for sequence comparison to LOS (AC# KT388101): LSS, *B. braunii* L race SS (AC# KT388100); BSS, *B. braunii* B race SS (AC# AH009227); AtSS, *Arabidopsis thaliana* SS (AC# D29017.1); YSS, yeast (*Saccharomyces cerevisiae*) SS (AC# M63979.1); HSS, human SS (AC# Q6IAX1).

Structure comparison. The LOS protein 3-D model was generated using the Iterative Threading ASSEmbly Refinement (I-TASSER) bioinformatics program[1-3]. Among five models of LOS predicted by I-TASSER, the model with a high confidence score (C-score = 0.19) was used for structural analysis in this study. The molecular graphics and structural analyses of the predicted LOS structure, the HSS crystal structure (PDB ID; 3WEF), and the CrtM crystal structure (PDB ID; 3AE0) were done using the UCSF Chimera package[4].

LOS expression vectors and LOS site-directed mutagenesis. The *6xHis-LOS$^{1-391}$* and *6xHis-LOS$^{33-381}$* expression constructs were generated by cloning *LOS* cDNA bases 1 to 1,173 and 97 to 1,143, respectively, into the *Nhe*I and *Hin*dIII restriction sites of pET28a[5]. The desired LOS point mutations were created using the *6xHis-LOS$^{1-391}$* background and primers containing the altered nucleotide sequence(s). Conditions for PCR-mediated site directed mutagenesis reaction using Pfu Turbo DNA Polymerase (Agilent Technologies) were as follows: 98°C initial denaturation for 2 min, 17 cycles of denaturation, annealing, and extension (98°C for 30 sec, 55°C

for 30 sec, 72°C for 8 min, respectively), and a final extension at 72°C for 10 min. All mutants were verified by DNA sequencing.

Protein expression and purification. The desired expression construct was transformed into *E.coli* BL21(DE3), and an overnight culture from a single colony was used to inoculate (1.7% v/v) 100 mL of TB medium. The culture was grown at 37°C to OD_{600} = 0.8, and protein expression induced by adding 1 mM isopropyl β-D-thiogalactoside. The induced cultures were then grown for an additional 6 hours at 25°C, cells harvested by centrifugation, and the pellets stored at -80°C for future use. Purification of the 6xHis tagged proteins was conducted using Ni-NTA agarose resin (QIAGEN) following the manufacture's recommendations with some modifications. All steps of purification were done either on ice or in a 4°C cold room. In a typical purification, the 100 mL culture pellet was suspended in 10 mL of lysis buffer (50 mM MOPS, pH=7.8, 300 mM NaCl, 10 mM imidazole, 1x general protease inhibitor cocktail (Sigma), 20 mM $MgCl_2$, 2.5 mM DTT, 1% glycerol (v/v)) followed by cell lysis using four successive probe sonications at 70% maximum power for 20 sec. The lysed samples were centrifuged at 16,000 x *g* for 30 min at 4°C, the supernatant incubated with 1 mL of pre-equilibrated Ni-NTA resin for 60 min at 4°C using a rocking table, the sample loaded into a gravity column, and the flow-through was discarded. The Ni-NTA column was washed with 10 mL of wash buffer (50 mM MOPS, pH=7.8, 300 mM NaCl, 60 mM imidazole, 20 mM $MgCl_2$, 2.5 mM DTT, 1% glycerol (v/v)), and the protein bound to the nickel resin was eluted with 2 mL of elution buffer (50 mM MOPS, pH=7.8, 300 mM NaCl, 400 mM imidazole, 20 mM $MgCl_2$, 2.5 mM DTT, 1% glycerol (v/v)). The eluted protein sample was dialyzed against storage buffer (50 mM MOPS, pH=7.8, 300 mM NaCl, 20 mM $MgCl_2$ and 5 mM DTT, 1% glycerol (v/v)), concentrated using an Amicon Ultra centrifugal filter (30kDa cutoff;

EMD Millipore) to the desired concentration, an equal volume of glycerol added, and the protein sample stored at -20°C for short term or at -80°C for future use.

Radioactive *in vitro* enzyme assays. The enzyme assays were conducted using the protocol described previously[5]. In brief, a 50 µL reaction was initiated by adding 1 µg of purified protein to a reaction buffer containing 50 mM MOPS, pH 6.8, 2.5 mM β-mercaptoethanol, 20 mM $MgCl_2$, 2 mM NADPH, and 10 µM of ^{3}H-prenyl-PP (0.125 µCi; specific activity = 0.25 Ci mmol^{-1}). For the mixed substrate assay 10 µM of both ^{3}H-FPP and ^{3}H-GGPP was used (0.125 µCi for each substrate; specific activity = 0.25 Ci mmol^{-1}). The specific activity for each substrate was adjusted by adding non-labeled FPP and/or GGPP. The reactions were incubated for 60 min at 37°C and terminated by adding 60µL of *n*-hexane, followed by brief vortexing and centrifugation. Thirty microliters of the supernatant was then analyzed on Silica gel 60 TLC plates using *n*-hexane as the mobile phase. ^{3}H incorporation into reaction products was determined by scraping the spots corresponding to authentic standards of lycopaoctaene (R_f= 0.09), $C_{35}H_{58}$ (R_f= 0.12) and squalene (R_f= 0.17) followed by an analysis on a liquid scintillation counter.

***EcDXS* and *EcFPS* cloning**. The cDNA sequences of *EcDXS* (AC# NP_414954) and *EcFPS* (a.k.a. ispA; AC# NP_414955) were obtained from the NCBI nucleotide database[6]. Genomic DNA from *E.coli* K-12 strain MG1655 and gene specific primers were used to amplify the PCR product using Phusion DNA polymerase followed by cloning into the pGEM-T vector (Promega). Gene specific primers were as follows: For *EcDXS*, forward primer 5'-ATGAGTTTTGATATTGCCAAATACCCG-3' and reverse primer 5'-TTATGCCAGCCAGGCCTTGATTTTG-3'; for *EcFPS*, forward primer 5'-ATGGACTTTCCGCAGCAACTC-3' and reverse primer 5'-TTATTTATTACGCTGGATGATGTAGTCCGC-3'.

***EcDXS*, *EcFPS*, and *AtGGPPS11* expression constructs**. The DNA template for *AtGGPPS11* was obtained from our previous study[5] and the DNA sequence encoding the 56 N-terminal chloroplast targeting signal amino acids was deleted to yield $AtGGPPS11^{57\text{-}371}$. The expression constructs were made using the following restriction sites and vectors: *EcDXS* in *Nde*I and *Xho*I of pET22b, *EcFPS* in *Bam*HI and *Sal*I of pACYDuet-1, and $AtGGPPS11^{57\text{-}371}$ in *Nde*I and *Xho*I of pACYDuet-1. For experiments involving expression of *Ec*FPS and *At*GGPPS11$^{57\text{-}371}$, the two cDNAs were expressed using a single expression construct, *EcFPS* + $AtGGPPS11^{57\text{-}371}$ in pACYDuet-1, by cloning *EcFPS* into the second multiple cloning site of $AtGGPPS11^{57\text{-}371}$:pACYDuet-1 using the *Bam*HI and *Sal*I restriction sites.

LOS *in vivo* mutant analysis in *E.coli*. The expression construct(s) described above were either transformed individually or in combination into *E.coli* BL21 (DE3) cells and the positive transformants were selected using standard procedures. The *E.coli* line harboring the desired construct(s) was grown in 60 mL of TB medium at 37°C to OD_{600} = 0.8, and gene expression was induced by adding 1mM isopropyl β-D-thiogalactoside. After induction, cells were grown for 6 hrs at 25°C, 50 mL of cells were harvested by centrifugation, the pellet snap frozen with liquid nitrogen, and the pellet lyophilized. Freeze-dried cells were transferred to a glass vial and extracted with *n*-hexane by vortexing vigorously at room temperature. The organic extracts were centrifuged at 1,000 x *g*, the supernatant dried, resuspended in 200 µL *n*-hexane, and a 5 µL aliquot analyzed by GC-MS.

GC-MS Analysis. A Bruker 436-GC-SCION SQ Premium GC-MS system was used to evaluate hydrocarbon production. GC-MS analyses were conducted using a 5% Phenyl BR-5ms capillary column (30 m × 0.25 mm, film thickness: 0.25 µm) in electron ionization (70 eV) mode using helium as a carrier gas at a flow rate of 2.58 mL min^{-1}. The initial oven temperature was held

at 220°C for 1 min followed by an increase in temperature at a rate of 5°C min^{-1} to 280°C, ramped again to 300°C at a rate of 2°C min^{-1}, and held for 20 min. The temperature for the injection port, the interface, and ion source were set at 280ºC, 250ºC, and 200ºC, respectively. Quantitation for hydrocarbon production in *E. coli* was done based on the calibration curve generated with commercially available squalene standard (Sigma).

References:

[1] Roy, A., Kucukural, A., and Zhang, Y. (2010) I-TASSER: a unified platform for automated protein structure and function prediction, *Nat. Protoc. 5*, 725-738.

[2] Roy, A., Yang, J. Y., and Zhang, Y. (2012) COFACTOR: an accurate comparative algorithm for structure-based protein function annotation, *Nucleic Acids Res. 40*, W471-W477.

[3] Zhang, Y. (2008) I-TASSER server for protein 3D structure prediction, *Bmc Bioinformatics 9*.

[4] Pettersen, E. F., Goddard, T. D., Huang, C. C., Couch, G. S., Greenblatt, D. M., Meng, E. C., and Ferrin, T. E. (2004) UCSF chimera - A visualization system for exploratory research and analysis, *J. Comput. Chem. 25*, 1605-1612.

[5] Thapa, H. R., Naik, M. T., Okada, S., Takada, K., Molnar, I., Xu, Y., and Devarenne, T. P. (2016) A squalene synthase-like enzyme initiates production of tetraterpenoid hydrocarbons in *Botryococcus braunii* Race L, *Nat. Commun. 7*, 11198.

[6] Blattner, F. R., Plunkett, G., Bloch, C. A., Perna, N. T., Burland, V., Riley, M., ColladoVides, J., Glasner, J. D., Rode, C. K., Mayhew, G. F., Gregor, J., Davis, N. W., Kirkpatrick, H. A., Goeden, M. A., Rose, D. J., Mau, B., and Shao, Y. (1997) The complete genome sequence of *Escherichia coli* K-12, *Science 277*, 1453-&.